

## Microstructural study of a discoloration process during in reaction bonding of silicon nitride

Kwan-ho Ko<sup>a</sup>, Kook-soo Bang<sup>a</sup>, Kwon-taek Lim<sup>b</sup>, Dong-soo Park<sup>c</sup>, Hai-doo Kim<sup>d</sup> and Chan Park<sup>a,\*</sup>

<sup>a</sup>Division of Materials Science & Engineering, Pukyong National University, Busan 608-739, Korea

<sup>b</sup>Division of Image Science and Engineering, Pukyong National University, Busan 608-739, Korea

<sup>c</sup>Department of Future Technology, Korea Institute of Machinery and Materials, Chang-Won 641-010, Korea

<sup>d</sup>Powder Materials Research Center, Korea Institute of Machinery and Materials, Chang-Won 641-010, Korea

An inhomogeneous coloration near the surface area of a RBSN (Reaction Bonded Silicon Nitride) sample proceeded due to an interaction between the gas atmosphere and silicon nitride. This unwanted non-uniform band formation of alpha silicon nitride was controlled using a graphite crucible, which resulted in a lower nitrogen partial pressure in the atmosphere. The reduced nitrogen partial pressure improved the nitridation rate up to 99% and successfully removed the grey coloration. By varying the nitrogen partial pressure in the atmosphere, a physical explanation for the discoloration in the grey-colored area could be given.

**Key words:** RBSN, Nitridation, Band formation, Coloration.

### Introduction

Reaction bonded silicon nitride ( $\text{Si}_3\text{N}_4$ ) materials have attracted interest because of an unusual feature associated with their fabrication and because of their promising thermo-mechanical properties. The nitridation of Si gives rise to a volume expansion up to 22%. The final density of RBSN is principally dependent on one parameter, the green density of the initial Si compacts, by contrast with most ceramics which shrink and are densified as they are fired. Consequently, this phenomenon is a great advantage when producing components with complex shapes and close dimensional tolerances. RBSN ceramics show a small shrinkage during the nitridation and the post sintering. This provides some advantages in controlling the dimension of products as well as reducing the price of the products.

The properties of RBSN can be affected by many processing variables [1-3]: the initial silicon particle size [4, 5], purity, and nitriding process, the composition, and pressure of the nitrogen-based gas ( $\text{N}_2+\text{H}_2$ ,  $\text{N}_2+\text{He}$ , added  $\text{O}_2$  or water vapor) [6-11], the pore size of compacts [12] and the compact size [13]. The nitridation reaction between Si and nitrogen in making silicon nitride is exothermic. Therefore, the nitriding schedule should be controlled carefully in order to avoid the fusion of silicon.

Goeb et al. [14] reported that a common feature of gas-pressure sintered silicon nitride ceramics was the inhomogeneous grey coloration of the near surface area. The same coloration was also observed for RBSN [15]. An interaction between the gas atmosphere and the material was responsible for the non-uniform coloration. The effect of the nitrogen partial pressure on the microstructure of reaction bonded silicon nitride was thermodynamically explained [16].

This paper describes a technique whereby reaction bonded silicon nitride can be processed to produce a high quality microstructure. Microstructural observations of the discoloration process during the reaction was also discussed.

### Experimental Procedure

A schematic diagram of the experimental procedure is presented in Fig. 1. The levels of nitridation were investigated as a function of the added static gas pressure. The average particle size of Si (Permascand Co. Grade 4) was 7  $\mu\text{m}$ . The impurity levels are given in Table 1.  $\text{Y}_2\text{O}_3$  (6 wt%) (Fine, H.C. Starck) and  $\text{Al}_2\text{O}_3$  (2 wt%) (AKP30, Sumitomo Chemical Co., Osaka, Japan) were used as sintering aids for post sintering. The starting materials were mixed in ethanol (PH=11) in an MC nylon jar after adding 5 wt% PEG (polyethylene glycol) as binder, and milled for 24 hours in a planetary ball mill with  $\text{Si}_3\text{N}_4$  balls as the milling media. In each case the resulting powder was dried and pressed to compact bodies.

The PEG binder was burnt out to enhance the pore channel distribution in the green compacts. After the

\*Corresponding author:  
Tel : +82-51-620-1650  
Fax: +82-51-624-0746  
E-mail: chanpark@pknu.ac.kr

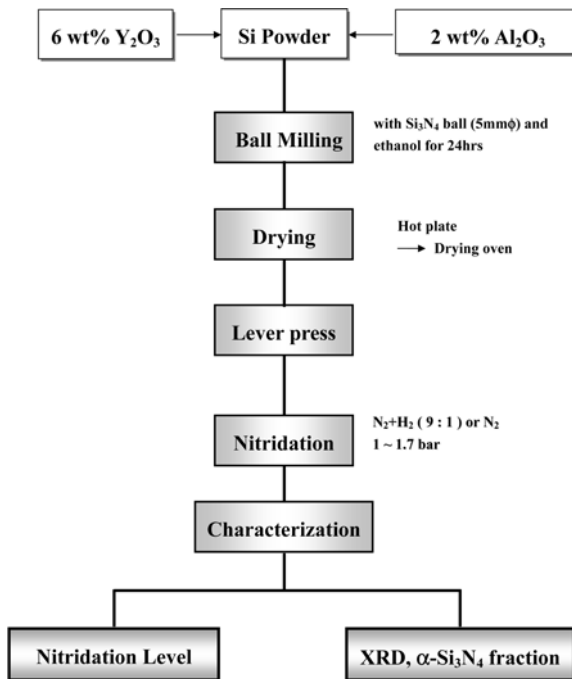


Fig. 1. Schematic diagram of the experimental procedure.

binder burn-out operation, the compacts were subjected to nitridation in either a  $N_2$ -10% $H_2$  gas mixture or in a  $N_2$  atmosphere. The samples were heated in a vacuum until the temperature reached  $300^\circ C$  and then the  $N_2$ - $H_2$  gas mixture was admitted to the desired pressure. At  $1300^\circ C$  the mixture was switched over to  $N_2$  gas. Figure 2 shows a schematic diagram of the computer-controlled nitriding furnace. In order to prevent reaction between the compact and graphite, and to minimize the contact area, the compacts were placed on BN coated silicon nitride balls. The level of nitridation after 26 hours reaction time was obtained from the following equation:

$$\text{Level of Nitridation (\%)} = 1.5(W - W_i) / W_{Si} \quad (1)$$

where  $W$  is the weight of the specimen after the nitridation reaction and  $W_i$  is the weight before nitridation,  $W_{Si}$  is the weight of Si before nitridation. The microstructural characteristics were studied by an optical microscope. Phase analysis was performed by XRD using  $Cu K_\alpha$  radiation and Ni a filter. The  $Si_3N_4$   $\alpha/\beta$  ratio after nitridation was calculated by the Gazarra and

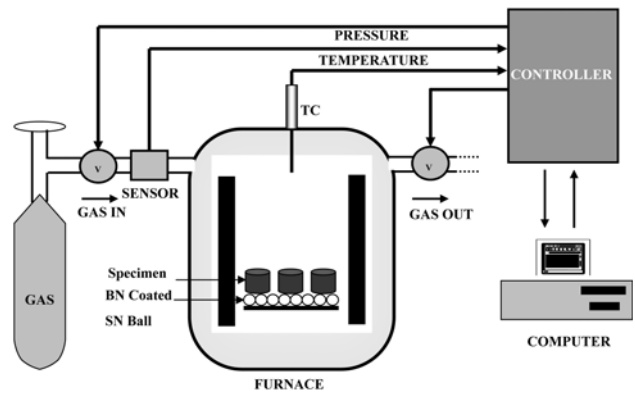


Fig. 2. Schematic diagram of the computer-controlled nitriding furnace.

Messier equation [17].

$$\alpha\text{-}Si_3N_4 = \frac{I_\alpha(210)/L_\alpha(210)}{I_\beta(210)/L_\beta(210) + I_\alpha(210)/L_\alpha(210)} \quad (2)$$

The cross sections of specimens which had various reaction levels were also examined to look for any coloration process produced by the nitridation reaction.

## Results and Discussion

Figure 3 shows photographs of the cross section of the specimens, which had various levels of nitridation. As the level of nitridation increased, the inhomogeneous coloration inside the specimen and/or near the surface proceeded due to the interaction between the gas atmosphere and the silicon nitride. Up to a level of 30% nitridation the specimen remained unchanged, showing a typical dark grey color all over the sample. From a level of 50% to 70% nitridation, the amount of silicon nitride increased, showing coloration of the near surface area and inside the specimen. When the level of nitridation reached 90%, the specimen color changed from dark grey (Si) to white grey ( $Si_3N_4$ ). Based on observations of the color, the sequences of the nitridation reaction with thickness were as follows; 1) The outside, 2) the inside, 3) an intermediate area of the specimen, indicating an easy penetration of the nitrogen gas into the inside of the specimen. The inhomogeneous coloration of  $Si_3N_4$  near the surface also proceeded

Table 1. Powders used in these experiments

	wt%	Manufacturer	Grade	Average Particle Size ( $\mu m$ )	Others
Si		Permascand, Sweden	4	7	Fe: 0.07% Al: 0.07% Ca: 0.01% C: 0.1% O: 0.2-1.0%
$Y_2O_3$	6	H.C. Starck Co., Germany	Fine	0.29	
$Al_2O_3$	2	Sumitomo Chemical Co., Japan	AKP30	0.37	

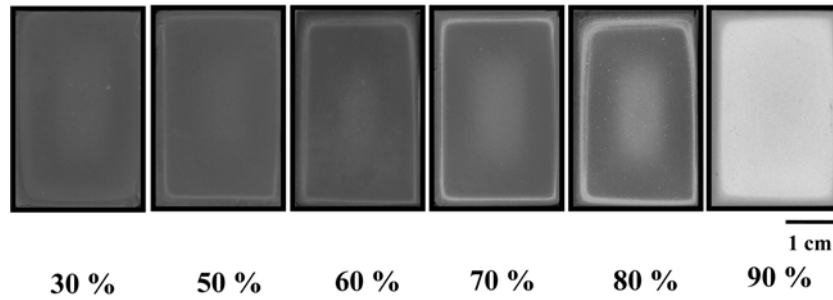


Fig. 3. Photographs of cross sections of the specimens which had various levels of nitridation (%).

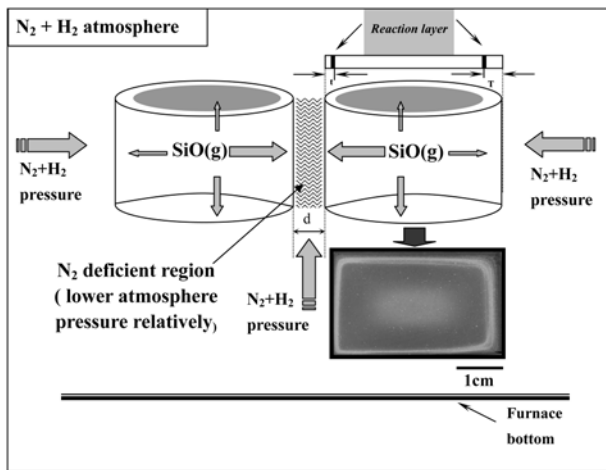
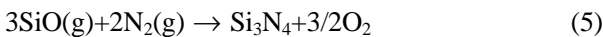
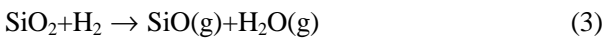


Fig. 4. Schematic diagram of the Si<sub>3</sub>N<sub>4</sub> layer formed near the surface of the specimen.

due to the interaction between the gas atmosphere and silicon. The formation of SiO was possible because the reaction between SiO<sub>2</sub> formed at the surface of the starting Si powder and H<sub>2</sub> in the gas mixture occurred in the early stage of nitridation (equation 3). SiO gas produced by this reactions reacted with N<sub>2</sub> gas to form alpha Si<sub>3</sub>N<sub>4</sub> or Si<sub>2</sub>N<sub>2</sub>O (equations 4, 5). It is believed that Si<sub>2</sub>N<sub>2</sub>O grows from a liquid phase which has been saturated with the dissolved nitrogen [18, 19]. This reaction (equation 5) was extensive at an early stage of nitridation due to more oxygen contamination in the starting materials :



There were more alpha crystals on the inside than at the outside of the specimen. The reaction temperature in the final stage of the nitridation reached above 1450 so that the amount of liquid glass was large enough to produce beta Si<sub>3</sub>N<sub>4</sub> at the surface of the small sample. Figure 4 shows a schematic diagram of the Si<sub>3</sub>N<sub>4</sub> layer formed near the surface of the specimen. Also an uneven Si<sub>3</sub>N<sub>4</sub> layer with a different thickness (as a function of time and temperatures t, T) was observed. The nitrogen partial pressure on each side of the speci-

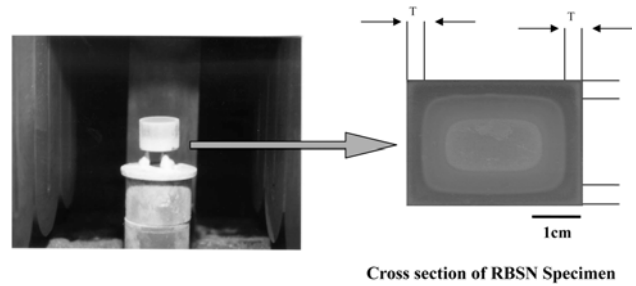


Fig. 5. Formation of α-Si<sub>3</sub>N<sub>4</sub> layer with a uniform thickness(T).

men was considerably different, resulting in a nitrogen-deficient region between specimens. In order to show the effect of the nitrogen partial pressure, only one specimen was placed in the center of the furnace and it clearly showed a uniform thickness of the Si<sub>3</sub>N<sub>4</sub> layer (Fig. 5). The fractions of α-Si<sub>3</sub>N<sub>4</sub> at different positions in the specimen are given in Fig. 6 and X-ray results of the specimen after nitridation to 70% are given in Fig. 7. This analysis was done from the surface to the center of the specimen (from A to F). The α/β Si<sub>3</sub>N<sub>4</sub> ratio was calculated based on equation (2). The (210) plane was selected to minimize the effect of grain size and the preferred orientation. A structure-related parameter (L) was obtained for each plane, and L<sub>α</sub> (210) and L<sub>β</sub> (210) were 6.79 and 11.21 respectively. A SiC peak was observed at the surface of the specimen, indicating there was a strong reaction between the Si powder and carbon in the atmosphere. In order to investigate the nitrogen partial pressure in the atmosphere, a graphite crucible was used. A total of 12 specimens were placed

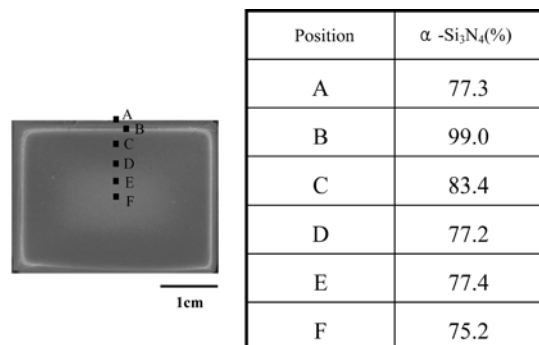
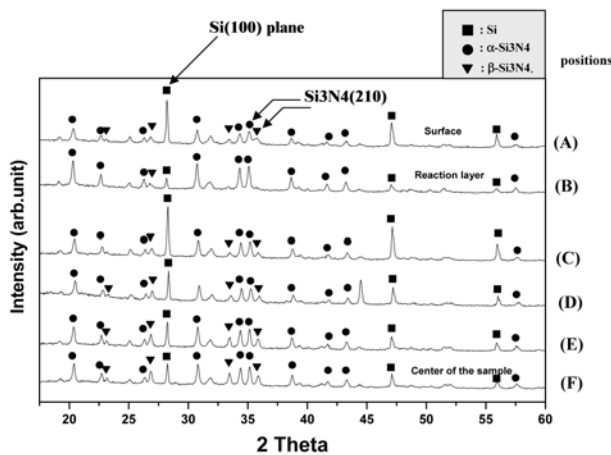
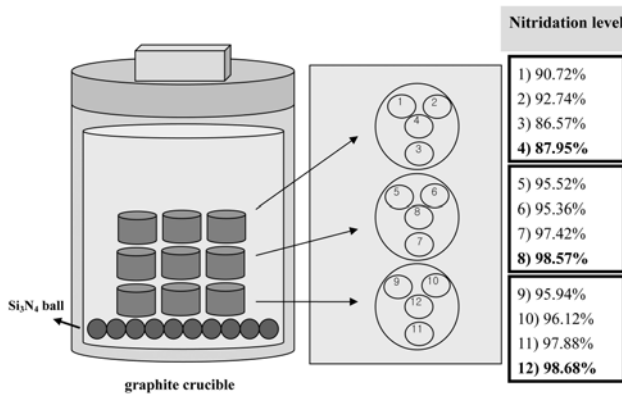


Fig. 6. The fractions of α-Si<sub>3</sub>N<sub>4</sub> at different positions.



**Fig. 7.** X-ray analysis of the specimen after 70% nitridation. The position A to F are shown on figure 6.



**Fig. 8.** The nitridation level for specimens placed at different positions.

on the silicon nitride balls. The nitridation levels for specimens placed at different positions are summarized in Fig. 8. This clearly indicates that the nitridation level of specimens in the nitrogen-deficient region reaches very high values up to 99%.

## Conclusions

Reaction bonded silicon nitride (RBSN) has been fabricated from Si powder with  $Y_2O_3$  and  $Al_2O_3$ . A computer controlled static nitriding system was constructed so that precise control of gas pressure and reaction temperature was obtained. A level of more than 90% nitridation was successfully obtained. The ratio of alpha ( $\alpha$ ) to beta ( $\beta$ ) silicon nitride was higher on the inside than that at the outside of the sample. The reaction temperature in the final stage of the nitridation reached above 1450°C so that the amount of liquid

glass was large enough to produce beta  $Si_3N_4$  at the surface. Uneven  $\alpha$ - $Si_3N_4$  layers were observed inside the samples since the nitrogen partial pressure at each side of the specimen were considerably different from each other. The unwanted non-uniform band formation of alpha silicon nitride was controlled using a graphite crucible, resulting in a lower nitrogen partial pressure in the atmosphere. The reduced nitrogen partial pressure improved the nitridation level up to 99% and successfully removed the grey coloration.

## Acknowledgement

This work was supported by Pukyong National University Research Fund in 2005.

## References

1. A.J. Moulson, *J. Mat. Sci.* 14 (1979) 1017-1051.
2. G. Ziegler, J. Heinrich, *J. Mat. Sci.* 22 (1987) 3041-3086.
3. F.L. Riley, *Materials Science Forum.* 47 (1989) 70-83.
4. A. Atkinson, A.J. Moulson, and E.W. Roberts, *J. Mater. Sci.* 10 (1975) 1242-1243.
5. R. Pompe, L. Hermansson, T. Johansson, E. Djurle and M.E. Hatcher, *Materials Science Engineering.* 71 (1985) 355-362.
6. D.P. Elias and M.W. Lindley, *J. Mater. Sci.* 11 (1976) 1278-1287.
7. H. Kim and C.H. Kim, *J. Mater. Sci. Lett.* 3 (1984) 199-200.
8. H. Kim and C.H. Kim, *J. Mater. Sci. Lett.* 3 (1984) 203-204.
9. J.Y. Park and C.H. Kim, *J. Kor. Ceram. Soc.* 23[5] (1986) 61-66.
10. Z. Jovanovic, S. Kimura, and O. Levenspiel, *J. Amer. Ceram. Soc.* 77[1] (1994) 186-192.
11. J. Heinrich, *Advanced Ceramic Materials.* 2[3A] (1987) 239-242.
12. J.L. Huang, S.W. Chen, H.H. Lu, and W.H. Chan, *Ceramics International.* 22 (1996) 27-31.
13. G.S. Hughs, C. Mcgreavy, and J.H. Merkin, *J. Mater. Sci.* 15 (1980) 2345-2353.
14. O. Goeb, M. Herrmann, S. Siegel, and P. Obenaus, *Key Engineering Materials* 132-136 (1997) 751.
15. D.S. Park, H.D. Kim, K.T. Lim, K.S. Bang, and Chan Park, *Materials Science and Engineering A* 405 (2005) 158-162.
16. Chan Park, K.S. Bang, K.T. Lim, D.S. Park, and H.D. Kim, *Solid State Phenomena* 121-123 (2007) 231-234.
17. C.P. Gazzara and D.R. Messier, *Ceram. Bull.* 56[9] (1977) 777-780.
18. I.A. Bondar and F.Y. Galakhov, *Izv. Akad SSSR, Ser. Khim.* 7 (1963) 1325.
19. M.E. Washburn, *Am. Ceram. Soc. Bull.* 46[7] (1967) 667.